

## Article

# Integer versus Fractional Order SEIR Deterministic and Stochastic Models of Measles

Md Rafiul Islam <sup>1,\*</sup> , Angela Peace <sup>1</sup>, Daniel Medina <sup>2</sup> and Tamer Oraby <sup>2</sup> 

<sup>1</sup> Department of Mathematics and Statistics, Texas Tech University, 2500 Broadway, Lubbock, Texas 79409; rafiul.islam@ttu.edu (M.R.I.); a.peace@ttu.edu (A.P.)

<sup>2</sup> School of Mathematical and Statistical Sciences, The University of Texas Rio Grande Valley, 1201 W. University Drive, Edinburg, Texas 78539; daniel.medina@utrgv.edu (D.M.); tamer.oraby@utrgv.edu (T.O.)

\* Correspondence: rafiul.islam@ttu.edu

**Abstract:** In this paper, we compare the performance between systems of ordinary and (Caputo) fractional differential equations depicting the susceptible-exposed-infectious-recovered (SEIR) models of diseases. In order to understand the origins of both approaches as mean-field approximations of integer and fractional stochastic processes, we introduce the fractional differential equations as approximations of some type of fractional nonlinear birth-death processes. Then, we examine validity of the two approaches against empirical courses of epidemics; we fit both of them to case counts of three measles epidemics that occurred during the pre-vaccination era in three different locations. While FDEs appear more flexible in fitting empirical data, our ODEs offered better fits to two out of three data sets. Important differences in transient dynamics between these modeling approaches are discussed.

**Keywords:** fractional SEIR stochastic model; Caputo fractional order differential equations; Measles; Parameter Estimation

## 1. Introduction

Modeling the spread of infectious diseases before the introduction of vaccines, as well as the validation of these models, has been widely studied since the works of Bernoulli [1], Ross [2], Brownlee [3], Greenwood and Yule [4], Kermack and McKendrick [5], Soper [6], Greenwood [7,8], M. S. Bartlett [9], Bailey [10]. See also Bailey [11] and Anderson [12] for more details about the history of disease modeling. Deterministic models using ordinary differential equations (ODEs) have received great attention [12–16] and wide assimilation by health sciences. See Temime *et al.* [17] and the references therein. Other deterministic models such as difference equations are also used to model the spread of diseases; for instance, see Fisman *et al.* [18]. However, fractional differential equations (FDEs) have been used in the last decade to model the course of epidemics [19–24].

Fractional differential equations are usually used to involve the memory of the process in the dynamics of the systems. There is more than one type of fractional order derivative; most notably, Caputo, Grünwald-Letnikov, and Riemann-Liouville [25]. Here, we study the Caputo fractional order derivative. Integer order derivatives of ordinary differential equations are special cases of fractional order derivatives. It was noted in more than one paper, e.g. [26], that FDEs give a better depiction of the courses of epidemics and natural phenomena than ODEs. Few researchers have fitted their FDE models to data [26,27], however, they lack details on justifying the goodness of fit so as to statistically validate them. This motivated us to compare systems of ODEs and FDEs by fitting them to some actual epidemic data.

Measles is a marker disease for virological, epidemiological, clinical, statistical, geographical, mathematical, and humanitarian reasons [28, p.16–21]. Mathematical modeling of measles epidemics

<sup>34</sup> dates as far as 1888 by D'Enko and then by Hamer [28, p.19]. Regularity and a large number of cases  
<sup>35</sup> of measles' epidemics with major peaks in the pre-vaccination era (before 1964) support the choice  
<sup>36</sup> of testing models against measles data. Many other researchers formulated measles models and fit  
<sup>37</sup> them to data, as in Bjørnstad *et al.* [29], where a time scale of two weeks is recommended fitting the  
<sup>38</sup> number of cases, and in Yingcun Xia *et al.* [30], where a model is used to examine a spatial network.  
<sup>39</sup> In this paper, we choose to use data of measles infections in the US and UK in two decades of the  
<sup>40</sup> pre-vaccination era (1944 – 1964), to compare the goodness of fit of ODEs and FDEs to those epidemics.

<sup>41</sup> While ordinary differential equations are well-established as deterministic models of the spread  
<sup>42</sup> of diseases (see e.g. Greenwood and Gordillo [31] and Vasilyeva *et al.* [32]), FDE models are sometimes  
<sup>43</sup> used. However, often these approaches lack mathematical basis or physical interpretation except  
<sup>44</sup> for exchanging integer differentiation with fractional ones, (see e.g. Almeida *et al.* [26] and Aranda  
<sup>45</sup> *et al.* [33]). Angstmann *et al.* [34] and Sardar *et al.* [35] provided a valid variation by considering the  
<sup>46</sup> memory of the non-Markovian infection process. The result is a mixed system of integer and fractional  
<sup>47</sup> derivatives of the Riemann-Liouville type. Saeedian *et al.* [36] showed how another memory functional  
<sup>48</sup> of the process can lead to replacing the integer derivatives with Caputo fractional derivatives. In this  
<sup>49</sup> paper, we show how Caputo fractional differential equations follow naturally from fractional stochastic  
<sup>50</sup> processes like those introduced in [37–46]. Then we show that for different data sets, FDE models fit  
<sup>51</sup> the data better for some epidemics whereas ODE models fit better for others. The Akaike Information  
<sup>52</sup> Criterion (AIC) and Bayesian Information Criterion (BIC) are used to compare between the fittings of  
<sup>53</sup> the two models to three data sets. For completeness, we will cover all the required background and the  
<sup>54</sup> relevant definitions in section 2. That includes a synopsis of Caputo's fractional calculus and fractional  
<sup>55</sup> stochastic SEIR processes. Section 2 will also include the derivation of the fractional order differential  
<sup>56</sup> equation depicting the SEIR model from the fractional stochastic SEIR process. It will be followed by  
<sup>57</sup> the stability analysis of the equilibria of the system of fractional differential equations, which will be  
<sup>58</sup> then fitted to measles data fitting and simulated.

## <sup>59</sup> 2. Methods

<sup>60</sup> In this section we provide a background for fractional differentiation and a fractional birth-death  
<sup>61</sup> process. We also introduce the integer and fractional differential equations for the SEIR model and  
<sup>62</sup> analyze the stability of the FDE's equilibria.

### <sup>63</sup> 2.1. Preliminaries

#### <sup>64</sup> 2.1.1. Fractional Calculus

Let  $D^n$  be the Leibniz integer-order differential operator given by

$$D^n f = \frac{d^n f}{dt^n} = f^{(n)},$$

and let  $J^n$  be an integration operator of integer order given by

$$J^n f(t) = \frac{1}{n!} \int_0^t (t - \tau)^{n-1} f(\tau) d\tau, \quad (1)$$

<sup>65</sup> where  $n \in \mathbb{Z}^+$ . Let us use  $D = D^1$  for the first derivative. We will use  $\partial_x^\alpha F := \frac{\partial^\alpha F}{\partial x^\alpha}$  and use  $\partial_x F := \frac{\partial F}{\partial x}$ .  
For fraction-order integrals, we use

$$J^{n-\alpha} f(t) = \frac{1}{\Gamma(n-\alpha)} \int_0^t (t - \tau)^{n-\alpha-1} f(\tau) d\tau, \quad (2)$$

where  $n - 1 < \alpha \leq n$ . Now, define the Caputo fractional differential operator  $D_*^\alpha$  to be,

$$D_*^\alpha f(t) = J^{n-\alpha} D^n f(t),$$

where  $n - 1 < \alpha \leq n$ , for  $n \in \mathbb{N}$ . It is also known that

$$\begin{aligned} \lim_{\alpha \rightarrow n} D_*^\alpha f(t) &= f^{(n)}(t), \\ \lim_{\alpha \rightarrow n-1} D_*^\alpha f(t) &= f^{(n-1)}(t) - f^{(n-1)}(0) \end{aligned} \quad (3)$$

for any  $n \in \mathbb{N}$ . We will consider  $n = 1$  in this work; that is  $0 < \alpha \leq 1$ . In that case,

$$J^{1-\alpha} f(t) = \int_0^t f(\tau) dg_t(\tau), \quad (4)$$

where  $g_t(\tau) = \frac{1}{\Gamma(2-\alpha)} (t^{1-\alpha} - (t-\tau)^{1-\alpha})$ . That is for each  $t$ , the integral  $J^{1-\alpha} f(t)$  is an area under  $f(\tau)$ , while above  $g_t(\tau)$  which works as a deformed or slowed time-scale as illustrated by Podlubny [47].

The generalized mean-value theorem for the Caputo fractional derivative is given as

$$f(x) = f(a) + \frac{1}{\Gamma(\alpha)} D_*^\alpha f(c)(x-a)^\alpha \text{ for some } a \leq c \leq x$$

and for all  $x \in (a, b]$  whenever  $f, D_*^\alpha f \in C([a, b])$ , see e.g. Özalp and Demirci [48].

The Mittag-Leffler is a function that generalizes the exponential function. That function can be written as follows,

$$E_\alpha(z) = \sum_{k=0}^{\infty} \frac{z^k}{\Gamma(\alpha k + 1)}, \quad \alpha \in \mathbb{R}^+, \quad z \in \mathbb{C}, \quad (5)$$

or, more generally using two parameters,

$$E_{\alpha,\beta}(z) = \sum_{k=0}^{\infty} \frac{z^k}{\Gamma(\alpha k + \beta)}, \quad \alpha, \beta \in \mathbb{R}^+, \quad z \in \mathbb{C}. \quad (6)$$

The general Mittag-Leffler has the following important property for any  $\alpha, \beta > 0$

$$E_{\alpha,\beta}(z) = z E_{\alpha,\alpha+\beta}(z) + \frac{1}{\Gamma(\beta)}. \quad (7)$$

Two important differential properties of the Mittag - Leffler function is that

$$D_*^\alpha e^{\lambda t} = t^{-\alpha} E_{1,1-\alpha}(\lambda t) \quad (8)$$

and

$$D_*^\alpha E_{\alpha,1}(\lambda t^\alpha) = \lambda E_{\alpha,1}(\lambda t^\alpha) \quad (9)$$

for any  $\lambda > 0$ .

## 2.2. Fractional Stochastic Process

Fix  $0 < \alpha \leq 1$ . Following Earn *et al.* [49], we consider a compartmental susceptible-exposed-infected-recovered (SEIR) model to depict the measles transmission dynamics in a closed population. Let  $X_1^{(\alpha)}, X_2^{(\alpha)}, X_3^{(\alpha)}$ , and  $X_4^{(\alpha)}$  be the number of susceptible, exposed, infected, and recovered individuals, respectively, such that  $X_1^{(\alpha)} + X_2^{(\alpha)} + X_3^{(\alpha)} + X_4^{(\alpha)} = N$ , the population size. Figure 1 shows how the disease is progressing from one sub-population to another.

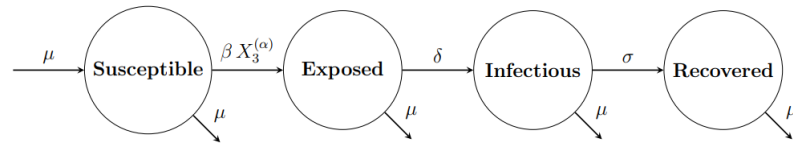


**Figure 1.** Schematic diagram of the SEIR model depicting transitions between different compartments.

78 Here,  $\mu$  is the recruitment and per capita death rate,  $\beta$  is the transmission rate,  $\delta$  is the rate at  
 79 which exposed individuals become infectious, and  $\sigma$  is the recovery rate.

80 A stochastic SEIR model can be depicted using a continuous time Markov chain (CTMC) like the  
 81 birth and death process with non-linear rates of transition as those given in table 1, see [50, p.22] and  
 82 [51, p.321]. M . S . Bartlett [9] and Greenwood and Gordillo [31] introduced (integer) stochastic SIR  
 83 model using CTMC with rates similar to those in the first six rows in table 1 to show a deterministic  
 84 SIR model of the ODE type depicting the approximate dynamics of the means of the processes. Here,  
 85 we introduce a fractional SEIR model using a CTMC of fractional birth and death process on triplets  
 86  $(i, j, k)$  with rates provided by table 1.

**Table 1.** Transitions and their rates for a birth and death process depicting a stochastic SEIR model.

Transition	Rate
$X_1^{(\alpha)} \rightarrow X_1^{(\alpha)} + 1$	$\mu N$
$X_1^{(\alpha)} \rightarrow X_1^{(\alpha)} - 1$	$\beta X_1^{(\alpha)} \frac{X_3^{(\alpha)}}{N} + \mu X_1^{(\alpha)}$
$X_2^{(\alpha)} \rightarrow X_2^{(\alpha)} + 1$	$\beta X_1^{(\alpha)} \frac{X_3^{(\alpha)}}{N}$
$X_2^{(\alpha)} \rightarrow X_2^{(\alpha)} - 1$	$(\mu + \delta) X_2^{(\alpha)}$
$X_3^{(\alpha)} \rightarrow X_3^{(\alpha)} + 1$	$\delta X_2^{(\alpha)}$
$X_3^{(\alpha)} \rightarrow X_3^{(\alpha)} - 1$	$(\mu + \sigma) X_3^{(\alpha)}$
$X_4^{(\alpha)} \rightarrow X_4^{(\alpha)} + 1$	$\sigma X_3^{(\alpha)}$
$X_4^{(\alpha)} \rightarrow X_4^{(\alpha)} - 1$	$\mu X_4^{(\alpha)}$

An  $\alpha$ -fractional SEIR stochastic process  $\{(X_1^{(\alpha)}(t), X_2^{(\alpha)}(t), X_3^{(\alpha)}(t)) : t \geq 0\}$  for  $0 < \alpha \leq 1$  with state probabilities

$$p_{(i,j,k)}^{(\alpha)}(t) = P((X_1^{(\alpha)}(t), X_2^{(\alpha)}(t), X_3^{(\alpha)}(t)) = (i, j, k) | (X_1^{(\alpha)}(0), X_2^{(\alpha)}(0), X_3^{(\alpha)}(0)) = (i_0, j_0, k_0))$$

87 for  $i, j, k = 0, 1, \dots$ , such that  $0 \leq i + j + k \leq N$  and  $P((X_1^{(\alpha)}(0), X_2^{(\alpha)}(0), X_3^{(\alpha)}(0)) = (i_0, j_0, k_0)) = 1$ ,  
 88 has a fractional forward Kolmogorov equation of the stochastic SEIR model similar to equation (A1)  
 89 and is given by

$$\begin{aligned}
 D_*^\alpha p_{(i,j,k)}^{(\alpha)}(t) &= \mu N p_{(i-1,j,k)}^{(\alpha)}(t) + \beta(i+1) \frac{k}{N} p_{(i+1,j-1,k)}^{(\alpha)}(t) + \mu(i+1) p_{(i+1,j,k)}^{(\alpha)}(t) \\
 &\quad + \delta(j+1) p_{(i,j+1,k-1)}^{(\alpha)}(t) + \mu(j+1) p_{(i,j+1,k)}^{(\alpha)}(t) + (\sigma + \mu)(k+1) p_{(i,j,k+1)}^{(\alpha)}(t) \\
 &\quad - (\mu N + \beta i) \frac{k}{N} + \mu i + (\delta + \mu) j + (\sigma + \mu) k p_{(i,j,k)}^{(\alpha)}(t)
 \end{aligned} \tag{10}$$

90 with  $p_{(i,j,k)}^{(\alpha)}(t) = 0$  if either  $i, j$ , or  $k$  are negative or more than  $N$ . See also Di Crescenzo *et al.* [45].  
 91 The classical forward Kolmogorov equation of the stochastic SEIR model follows when  $\alpha = 1$  with  
 92 state probabilities  $p_{(i,j,k)}^{(1)}(t)$ , [51, p.321]. Equation (10) can be used to find the probability generating

93 function  $G^{(\alpha)}(u, v, w, t) = E(u^{X_1^{(\alpha)}(t)} v^{X_2^{(\alpha)}(t)} w^{X_3^{(\alpha)}(t)})$  of the state probabilities, as the solution of the  
 94 Cauchy problem

$$\begin{aligned} D_*^\alpha G^{(\alpha)} &= \mu N(u-1)G^{(\alpha)} + \mu(1-u)\partial_u G^{(\alpha)} + (\delta w + \mu - (\delta + \mu)v)\partial_v G^{(\alpha)} \\ &\quad + (\sigma + \mu)(1-w)\partial_w G^{(\alpha)} + \beta \frac{w}{N}(v-u)\partial_{uw} G^{(\alpha)} \end{aligned} \quad (11)$$

95 for  $t > 0$  and  $G^{(\alpha)}(u, v, w, 0) = u^{i_0} v^{j_0} w^{k_0}$ , for  $-1 < u, v, w < 1$ .

96 Note that, the integer or classical stochastic SEIR process is  $(X_1^{(1)}(t), X_2^{(1)}(t), X_3^{(1)}(t))$  which is  
 97 simply the case when  $\alpha = 1$ . But that leads to another interesting fact that defines the relationship  
 98 between the fractional and integer stochastic SEIR model; that is, the former process is a random-time  
 99 subordination of the latter one, as established for other fractional processes like the fractional Poisson  
 100 process [37,45,52], and the fractional birth and/or death processes [39,40,42,43,53].

**Theorem 1.** *The fractional stochastic SEIR process  $(X_1^{(\alpha)}(t), X_2^{(\alpha)}(t), X_3^{(\alpha)}(t))$  has the same distribution as the random-time subordinated integer stochastic SEIR process*

$$(X_1^{(1)}(\mathcal{T}_{2\alpha}(t)), X_2^{(1)}(\mathcal{T}_{2\alpha}(t)), X_3^{(1)}(\mathcal{T}_{2\alpha}(t)))$$

101 for  $t > 0$  and  $0 < \alpha \leq 1$ .

102 The proof is provided in Appendix A.

### 103 2.3. Measles' Model via Fractional Differential Equations (FDE)

The means of the three discrete-marginal processes  $X_1^{(\alpha)}(t)$ ,  $X_2^{(\alpha)}(t)$ , and  $X_3^{(\alpha)}(t)$  can be found using  $\partial_u G^{(\alpha)}(1, 1, 1, t)$ ,  $\partial_v G^{(\alpha)}(1, 1, 1, t)$ , and  $\partial_w G^{(\alpha)}(1, 1, 1, t)$ , respectively. Let  $S^{(\alpha)}(t) := \frac{1}{N}E(X_1^{(\alpha)}(t))$ ,  $E^{(\alpha)}(t) := \frac{1}{N}E(X_2^{(\alpha)}(t))$ , and  $I^{(\alpha)}(t) := \frac{1}{N}E(X_3^{(\alpha)}(t))$ , where  $N$  is the total population size and  $E(x)$  is the expected value of  $x$ . Thus using equation (11), and approximating  $E(X_1^{(\alpha)}(t)X_3^{(\alpha)}(t))$  by  $E(X_1^{(\alpha)}(t))E(X_3^{(\alpha)}(t))$  we reach the fractional order version of the system of equations that was used by M. S. Bartlett [9] to model measles,

$$\begin{aligned} D_*^\alpha S^{(\alpha)} &= \mu - \beta S^{(\alpha)} I^{(\alpha)} - \mu S^{(\alpha)} \\ D_*^\alpha E^{(\alpha)} &= \beta S^{(\alpha)} I^{(\alpha)} - (\mu + \delta)E^{(\alpha)} \\ D_*^\alpha I^{(\alpha)} &= \delta E^{(\alpha)} - (\mu + \sigma)I^{(\alpha)} \end{aligned} \quad (12)$$

where  $S^{(\alpha)}$ ,  $E^{(\alpha)}$ , and  $I^{(\alpha)}$  be the proportion of susceptible, exposed, and infected individuals, respectively. With proportion of recovered individuals given by  $R^{(\alpha)} = 1 - (S^{(\alpha)} + E^{(\alpha)} + I^{(\alpha)})$ , we reach the fractional  $\alpha$  order SEIR model

$$\begin{aligned} D_*^\alpha S^{(\alpha)} &= \mu - \beta S^{(\alpha)} I^{(\alpha)} - \mu S^{(\alpha)} \\ D_*^\alpha E^{(\alpha)} &= \beta S^{(\alpha)} I^{(\alpha)} - (\mu + \delta)E^{(\alpha)} \\ D_*^\alpha I^{(\alpha)} &= \delta E^{(\alpha)} - (\mu + \sigma)I^{(\alpha)} \\ D_*^\alpha R^{(\alpha)} &= \sigma I^{(\alpha)} - \mu R^{(\alpha)} \end{aligned} \quad (13)$$

with  $0 < \alpha \leq 1$ . The non-negative parameters  $\beta$ ,  $\mu$ ,  $\delta$ , and  $\sigma$  – denoting them by  $\theta$ , for brevity – have dimensions given by  $\frac{1}{\text{time}^\alpha}$ . By construction of the FDE model as a mean field approximation of the  $\alpha$ -fractional stochastic SEIR process which in its turn is a subordination of an integer stochastic SEIR process by Theorem 1, those parameters could be interpreted as the rates measured by an independent observer of the process or calculated based on a cosmic time flow [47]. We replace those parameters

with a power  $\alpha$  of new parameters; that is,  $\theta_*^\alpha$  in place of  $\theta$  so the parameters  $\theta_*$  will have the dimension of  $\frac{1}{\text{time}}$  and the system becomes the following form:

$$\begin{aligned} D_*^\alpha S^{(\alpha)} &= \mu_*^\alpha - \beta_*^\alpha S^{(\alpha)} I^{(\alpha)} - \mu_*^\alpha S^{(\alpha)} \\ D_*^\alpha E^{(\alpha)} &= \beta_*^\alpha S^{(\alpha)} I^{(\alpha)} - (\mu_*^\alpha + \delta_*^\alpha) E^{(\alpha)} \\ D_*^\alpha I^{(\alpha)} &= \delta_*^\alpha E^{(\alpha)} - (\mu_*^\alpha + \sigma_*^\alpha) I^{(\alpha)} \\ D_*^\alpha R^{(\alpha)} &= \sigma_*^\alpha I^{(\alpha)} - \mu_*^\alpha R^{(\alpha)} \end{aligned} \quad (14)$$

#### 104 2.4. Measles' Model via Ordinary Differential Equations (ODE)

105 The following system of differential equations represents the ordinary differential equation  
 106 representation of the SEIR model and is the FDE model when  $\alpha = 1$  in equation 14.

$$\begin{aligned} DS &= \mu - \beta SI - \mu S \\ DE &= \beta SI - (\mu + \delta) E \\ DI &= \delta E - (\mu + \sigma) I \\ DR &= \sigma I - \mu R \end{aligned} \quad (15)$$

107 where  $\mu, \beta, \delta$ , and  $\sigma$  are the model parameters described above. They all have dimensions given by  
 108  $\frac{1}{\text{time}}$ . The last equation in (15) is redundant since  $R = 1 - (S + E + I)$ .

#### 109 2.5. Measles' Model via $\alpha$ -dependent Ordinary Differential Equations

110 We are interest in comparing the FDE vs ODE modeling approaches. It is important to note that  
 111 the basic ODE case considers  $\alpha = 1$ , however in the FDE case,  $\alpha$  appears in the derivative as well as the  
 112 parameter values. In order to better compare these two approaches, here we develop an ODE analogue  
 113 to the FDE that incorporates  $\alpha$  in the parameter values. We call this new system the  $\alpha$ -dependent ODE.  
 114 By dropping the  $\alpha$  order derivative from the left side and  $\alpha$  power from  $S^{(\alpha)}$ ,  $E^{(\alpha)}$ , and  $I^{(\alpha)}$  of equation  
 115 (14), our  $\alpha$ -dependent ODE takes the following form:

$$\begin{aligned} DS &= \mu_*^\alpha - \beta_*^\alpha SI - \mu_*^\alpha S \\ DE &= \beta_*^\alpha SI - (\mu_*^\alpha + \delta_*^\alpha) E \\ DI &= \delta_*^\alpha E - (\mu_*^\alpha + \sigma_*^\alpha) I \\ DR &= \sigma_*^\alpha I - \mu_*^\alpha R \end{aligned} \quad (16)$$

#### 116 2.6. Model Analysis

117 Analysis of the ODE is almost the same as of the FDE so we include the FDE one here. We start by  
 118 proving the positive invariance of the region of solutions of the FDE model. Henceforth, we drop the  $\alpha$   
 119 from  $S^{(\alpha)}$ ,  $E^{(\alpha)}$ , and  $I^{(\alpha)}$ , for brevity.

120 The following two lemmas of asymptotic behavior of FDEs are given here and their proof in  
 121 appendix A for completeness.

122 **Lemma 1.** *The closed simplex region  $M = \{(S, E, I) \in \mathbb{R}_+^3 : 0 \leq S + E + I \leq 1\}$  is a positive invariant set  
 123 for the FDE model in (14).*

124 We can find the model's equilibrium points by setting  $D_*^\alpha S = 0$ ,  $D_*^\alpha E = 0$ , and  $D_*^\alpha I = 0$ . Thus,  
 125 there are two equilibria to the measles' SEIR model (14). They are:

126 1. the disease free equilibrium  $DFE \equiv (1, 0, 0)$ , and

## 2. the endemic equilibrium

$$EE = (s^*, e^*, i^*) \equiv \left( \frac{1}{R_0}, \frac{\mu}{\delta + \mu} \left( 1 - \frac{1}{R_0} \right), \frac{\mu}{\beta} (R_0 - 1) \right).$$

127 where the basic reproduction number is  $R_0 := \frac{\beta\delta}{(\mu+\sigma)(\mu+\delta)}$ .  $EE$  exists only when  $1 < R_0 < 1 + \frac{\beta}{\mu}$ .

128 An equilibrium is locally asymptotically stable if the eigenvalues of the Jacobian matrix of the  
 129 n-dimensional system, namely  $\lambda_1, \lambda_2, \dots, \lambda_n$ , have the property that  $|\arg(\lambda_i)| > \frac{\alpha\pi}{2}$ , for  $i = 1, 2, \dots, n$ ,  
 130 [25, p.158]. Thus, in general, the stability of the ordinary differential equations model implies stability  
 131 of its fractional counter model. But, here they are equivalent due to the following lemma whose  
 132 solution could be found in appendix A.

133 **Lemma 2.** *The Disease-Free Equilibrium DFE is locally asymptotically stable if  $R_0 < 1$ . The endemic  
 134 equilibrium EE is locally asymptotically stable if  $R_0 > 1$ .*

135 Therefore, they have the same asymptotic behavior. Yet, the transient behavior differs as will be  
 136 seen by simulations below.

Moreover, a very important difference is their oscillation behavior is not similar. Let  $\lambda_\ell$  and  $u_\ell$  for  
 $\ell = 1, 2, \dots, N$  be the eigenvalues and their respective eigenvectors of an  $N \times N$  matrix  $A$ . The general  
 solution of initial value problem consisting of a system of  $N$  linear fractional differential equations  
 $D_*^\alpha x(t) = Ax(t)$  such that  $x(0) = x_0$  can be found to be

$$x(t) = \sum_{\ell=1}^N c_\ell u_\ell E_\alpha(\lambda_\ell t^\alpha) \quad (17)$$

for certain constants  $c_\ell \in \mathbb{C}$  for  $\ell = 1, 2, \dots, N$  such that  $\sum_{\ell=1}^N c_\ell u_\ell = x_0$ , [25, Theorem 7.13]. In case  
 that  $\alpha = 1$ , we recover the known solution of the system of ODEs given by

$$x(t) = \sum_{\ell=1}^N c_\ell u_\ell \exp(\lambda_\ell t).$$

137 If  $N = 3$  and  $A$  is not a symmetric matrix then at least one of the eigenvalues is a real-valued number  
 138 and the other two eigenvalues, say  $\lambda_2$  and  $\lambda_3$ , are conjugate complex-valued. In that situation,  $x(t)$   
 139 would oscillate with inter-peak periods, called inter-epidemic period in disease modeling, given by  
 140  $2\pi(\Im(\lambda_2))^{-1}$  [14]. If  $\Re(\lambda_\ell) < 0$  for all  $\ell$  then the oscillations will be damped to zero. That damped  
 141 oscillation is clear in the case of  $\alpha = 1$  due to the exponential damping in the superposition of the sine  
 142 and cosine functions. That behavior, however, is not straight forward for  $0 < \alpha < 1$ .

### 143 2.7. Numerical Simulations

Since the mean of the subordinator process is  $E(\mathcal{T}_\alpha(t)) = \frac{t^\alpha}{\Gamma(\alpha + 1)}$ , we use a method similar to  
 that was introduced in Demirici and Özalp [54] to find approximate solutions to initial value FDE  
 problems. We use that method here to simulate the solution of the FDE measles SEIR model. Consider  
 the initial value problem

$$\begin{aligned} D_*^\alpha x(t) &= f(t, x(t)), \text{ for } 0 < t \leq T, \\ x(0) &= x_0, \end{aligned} \quad (18)$$

for some  $T > 0$ . A solution of (18) is approximated by the deterministic time subordination

$$x(t) = y \left( \frac{t^\alpha}{\Gamma(\alpha + 1)} \right), \quad (19)$$

of  $y(s)$ , the solution of the ordinary differential equation

$$\frac{dy(s)}{ds} = g(s, y(s)), \text{ for } 0 < s \leq \frac{t^\alpha}{\Gamma(\alpha + 1)} \quad (20)$$

$$y(0) = x_0.$$

where

$$g(s, y(s)) = f(t - (t^\alpha - s\Gamma(\alpha + 1))^{\frac{1}{\alpha}}, x(t - (t^\alpha - s\Gamma(\alpha + 1))^{\frac{1}{\alpha}})). \quad (21)$$

<sup>144</sup> for all  $0 < t \leq T$ , [54].

<sup>145</sup> We use the subordination of the solution of ODEs to FDEs represented in equations (19) and (20)  
<sup>146</sup> to numerically simulate solutions of FDEs, see algorithm 1.

---

**Algorithm 1** Numerical solution of  $D_*^\alpha x(t) = f(t, x(t))$  for  $0 < t < T$  with  $x(0) = x_0$ .

---

Input:  $\alpha, T, f(t, x(t)), m, n$  Output:  $x(t)$

**begin**

Divide the interval  $[0, T]$  into  $n$  sub-intervals using

$$0 = t_0 < t_1 < \dots < t_n = T.$$

**for**  $i = 1, 2, \dots, n$

Divide the interval  $[0, \frac{t_i^\alpha}{\Gamma(\alpha + 1)}]$  into further  $m$  sub-intervals using

$$0 = s_0 < s_1 < \dots < s_m = \frac{t_i^\alpha}{\Gamma(\alpha + 1)}.$$

Solve the system  $Dy(s) = f(t_i - (t_i^\alpha - s\Gamma(\alpha + 1))^{\frac{1}{\alpha}}, y(s))$  with  $y(0) = x_0$  using Euler or Runge-Kutta methods on  $s_0, s_1, \dots, s_m$ .

Retain  $x(t_i) = y(s_m)$ .

**end**

Return  $[x_0, x(t_1), x(t_2), \dots, x(t_n)]$ .

**end**

---

<sup>147</sup> 2.8. Fitting FDE and ODE models to measles data

We use the method of ordinary least squares (OLS) to fit the FDE model to the data by minimizing the objective function

$$L(\alpha, \beta, \mu, \delta, \sigma) = \sum_{i=1}^n (I_i^{(d)} - I_i^{(s)})^2$$

<sup>148</sup> for  $\alpha \in (0, 1]$ , and  $\beta, \mu, \delta, \sigma \in (0, \infty)$ , where  $I^{(d)}$  is the data of actual proportion of infections and  $I^{(s)}$  is  
<sup>149</sup> the simulated proportion of infections. The values  $I_i^{(s)}$  approximating  $I(t_i)$  are found by solving the  
<sup>150</sup> FDE model using algorithm 1.

<sup>151</sup> Parameter estimation was conducted using Matlab MultiStart and fmincon functions. MultiStart  
<sup>152</sup> carries out the optimization procedure using initial points within the parameters' spaces. It generates  
<sup>153</sup> some initial points depending on a converging algorithm. The fmincon finds a local minimum for the  
<sup>154</sup> constrained nonlinear multivariable function. The MultiStart together with fmincon do the global  
<sup>155</sup> optimization of a nonlinear multivariable function. The MultiStart function uses parallel processing  
<sup>156</sup> which drastically reduces the running time.

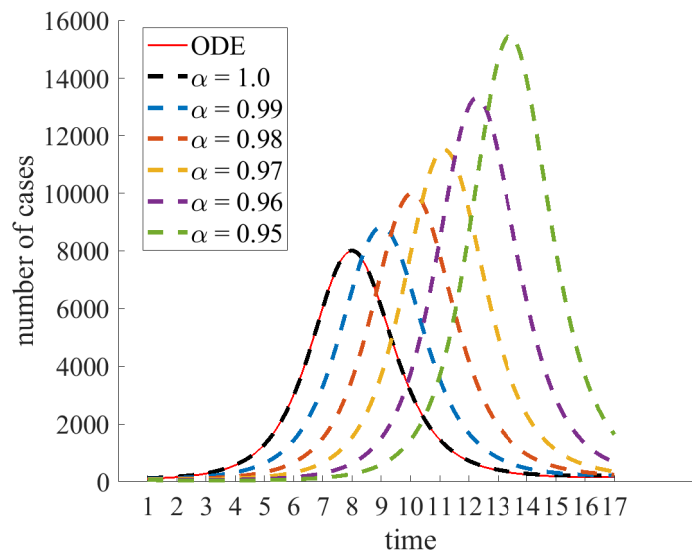


**Figure 2.** Number of cases using classical ODE model and FDE model with different fractional orders  $\alpha$ . The simulations are done using  $\mu = \mu_* = 0.0027$ ,  $\beta = \beta_* = 119.2257$ ,  $\delta = \delta_* = 16.7301$ , and  $\sigma = \sigma_* = 10.1873$ .

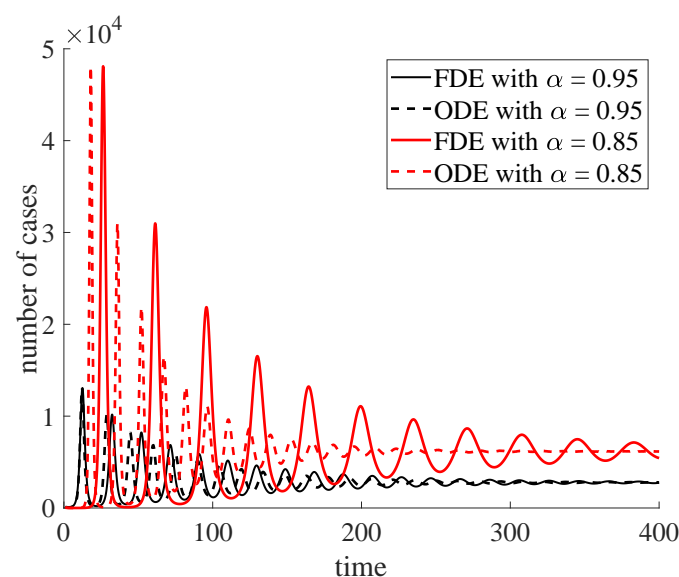


**Figure 3.** Number of cases using FDEM and its analogous ODEM with different fractional orders  $\alpha$ . The simulations are done using  $\mu_* = 0.0027$ ,  $\beta_* = 119.2257$ ,  $\delta_* = 16.7301$ , and  $\sigma_* = 10.1873$ .

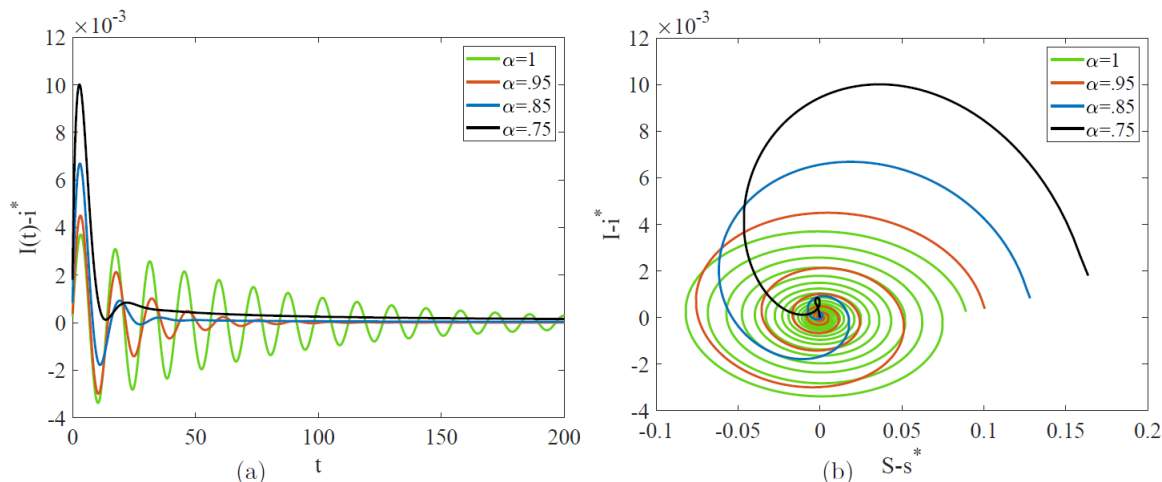


**Figure 4.** Simulations of solutions of the SEIR FDE centered about the endemic equilibrium (EE) for  $\alpha = 1, .95, .85$ , and  $.75$  using equation (17) shows a suppression of damped oscillations as  $\alpha$  decreases. The simulations are done using  $\mu_\star = 0.0027$ ,  $\beta_\star = 119.2257$ ,  $\delta_\star = 16.7301$ , and  $\sigma_\star = 10.1873$ .

### 157 3. Results

158 We solve the system of FDE (equation 14) using algorithm 1 and the systems of ODE (equations  
 159 15 and 16) using the Runge-Kutta method.

160 Simulations of the classical ODE (equation 15) and FDE (equation 14), Figure 2, shows that  
 161 the system of fractional differential equations is very sensitive to its order of differentiation  $\alpha$ . For  
 162 smaller  $\alpha$ , the peak number of cases of the epidemic is larger but the duration of the outbreak is  
 163 shorter. The solution of the FDE model converges to the solution of the classical ODE as  $\alpha \rightarrow 1$ . To  
 164 further compare the two modeling approaches, we consider the analogue ODEs derived for specific  $\alpha$   
 165 values, see equation (16). These comparisons are shown in Figure 3. During transient dynamics both  
 166 models exhibit several peaks in the number of cases. The number of these peaks and their respective  
 167 amplitudes are similar between models, however there are differences in the timing of these peaks.  
 168 The transient oscillations of the FDE model are more stretched out than its ODE analogue, and its  
 169 solutions experience longer inter-epidemic times. Both models approach the same equilibria solutions.

170 Simulations of equation (17) in Figure 4 shows that disease models of fractional order equations  
 171 lack the same oscillatory behavior exhibited by systems of ODEs with conjugate complex eigenvalues  
 172 of the Jacobian matrices calculated at endemic equilibrium.

173 The models were fitted to three measles' epidemics in the pre-vaccination era in three different  
 174 cities: New York, London, and Portsmouth. Simulations of the fitted ODE and FDE models are  
 175 shown in Figure 5. See also Appendix B for the data and the parameter estimates. The estimate  
 176 of  $\alpha$  are 0.99, 0.99, and 0.88 for New York, London, and Portsmouth respectively. The AIC and BIC  
 177 are found to be smaller for ODE models for the epidemics in New York and London with values of  
 178 AIC(ODE)= 250.539 and 389.358 and BIC(ODE)= 253.872 and 394.541, respectively, while AIC(FDE)=  
 179 255.360 and 413.275 and BIC(FDE)= 259.526 and 419.754, respectively. For Portsmouth's epidemic, the  
 180 results are the opposite, AIC(ODE)= 277.938 and BIC(ODE)= 282.978 while AIC(FDE)= 271.920 and  
 181 BIC(FDE)= 278.213. Yet the differences between the fitting of ODE and FDE models are not striking.

### 182 4. Discussion

183 Replacing first order derivatives with Caputo fractional derivatives has been the practice for  
 184 many studies using fractional order modeling of diseases. In this paper, we show how those models  
 185 follow from an approximation to the dynamical system governing the means of fractional stochastic  
 186 SEIR processes. Moreover, we study ordinary and fractional order systems of differential equations  
 187 of SEIR models using three data sets of measles epidemics in three different cities selected from the

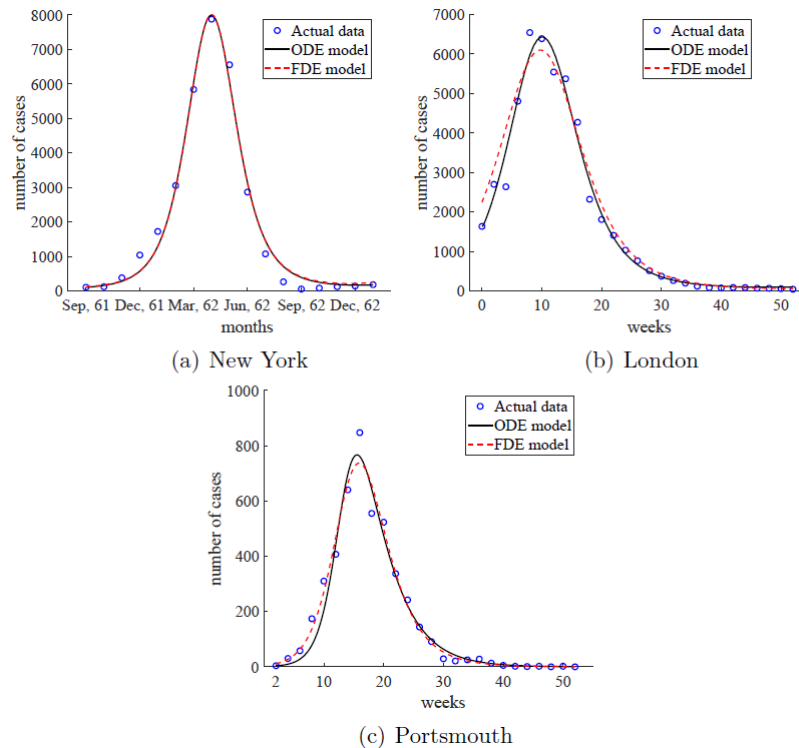


**Figure 5.** Simulations of ODE and FDE models fitted to measles epidemics in the pre-vaccination era.

188 pre-vaccination era. It appears that, in some situations, the fractional order differential equation model  
 189 (FDEM) gives better fit than the ordinary differential equation model (ODEM).

190 Angstmann *et al.* [34] use the master equation of a continuous-time random walk to derive an  
 191 FDEM involving Riemann-Liouville fractional derivatives. Power laws are postulated to model time of  
 192 infectiousness and recovery. That extension from exponential times in ordinary differential equations  
 193 is a different approach from the mean field approximation of a stochastic process. Saeedian *et al.* [36]  
 194 introduced the Caputo fractional differential equations through a memory of the whole process of  
 195 infection and disease recovery. In our paper, we have considered, for the first time, fractional stochastic  
 196 SEIR model and have shown how the Caputo fractional differential equations follows as mean-field  
 197 approximation of the process.

198 Fractional stochastic SEIR model introduced here turns out to be a random-time subordination  
 199 of a classical stochastic SEIR model. Other real-life systems are modeled using a subordination of a  
 200 stochastic process. A subordinated process was introduced by Mandelbrot and Taylor [55] to model  
 201 the logarithm of market prices where the original process is a Brownian motion subordinated by a  
 202 stochastic time process  $\mathcal{T}_{2\alpha}$ , which is the same random time process we have found here. In Mandelbrot  
 203 and Taylor [55], the stochastic time process  $\mathcal{T}_{2\alpha}$  is called the operational time and  $t$  is the physical time.

204 Further study of the fractional stochastic SEIR model might lead to interesting dynamical  
 205 behaviors. For instance, it can provide more insights into the stochastic oscillations of the disease in  
 206 a more flexible way than their classical counterparts. Thus, studying the fractional stochastic SEIR  
 207 model is the next step in this work.

## 208 5. Conclusion

209 In this paper, we compare two deterministic models of disease: ordinary differential equations  
 210 (ODE) and fractional differential equations (FDE). We use three different data sets of measles epidemics  
 211 from the pre-vaccination era. We also explain FDEs as the mean-field approximation of a fractional

212 stochastic SEIR model. Up to our knowledge, this is the first time such a fractional stochastic process is  
 213 introduced and connected to the fractional order differential equations.

214 While ODE models are regularly used to model epidemics, such as measles, FDEs seem to have  
 215 the potential to offer improved model fitting. Rates of transition between compartments in that case  
 216 could be interpreted as rates with respect to an external observer with a different type of clock, may be  
 217 due to delay in reporting.

218 **Author Contributions:** Conceptualization, M.R.I., A.P. and T.O.; methodology, M.R.I., D.M. and T.O.; software,  
 219 M.R.I. and T.O.; validation, M.R.I. and T.O.; formal analysis, M.R.I. and T.O.; investigation, M.R.I. and T.O.; data  
 220 curation, M.R.I. and T.O.; writing—original draft preparation, M.R.I., D.M., A.P. and T.O.; writing—review and editing,  
 221 M.R.I., A.P. and T.O.; visualization, M.R.I., A.P., D.M. and T.O.; supervision, A.P. and T.O.; funding acquisition, A.P.

222 **Funding:** A.P. was partially supported by NSF grant DMS-1815750.

223 **Acknowledgments:** We thanks Joshua Padgett for his valuable comments.

224 **Conflicts of Interest:** The authors declare that they have no competing interests. The funders had no role in the  
 225 design of the study; in the collection, analyses, or interpretation of data; in the writing of the manuscript, or in the  
 226 decision to publish the results.

## 227 Appendix A. Some Definitions and Proofs

Laplace transform of a function  $f(t)$  is defined as

$$\mathcal{L}(f)(s) = \hat{f}(s) = \int_0^\infty e^{-st} f(t) dt.$$

The inverse transform is defined by

$$\mathcal{L}^{-1}(\hat{f})(t) = \frac{1}{2\pi i} \int_{\mathcal{C}} e^{st} \hat{f}(s) ds$$

where  $\mathcal{C}$  is a contour parallel to the imaginary axis and to the right of the singularities of  $\hat{f}$ . The Laplace transform of the Caputo fractional derivative is given by

$$\mathcal{L}(D_*^\alpha f)(s) = s^\alpha \hat{f}(s) - s^{\alpha-1} f(0).$$

228 **Fractional Birth and Death Process:**

An  $\alpha$ -fractional nonlinear birth and death process  $\{N_\alpha(t) : t \geq 0\}$  for  $0 < \alpha \leq 1$  with state probabilities

$$p_n^\alpha(t) = P(N_\alpha(t) = n | N_\alpha(0) = 1)$$

for  $n \geq 0$  is defined through the forward Kolmogorov (difference-)differential equations

$$D_*^\alpha p_n^\alpha(t) = \lambda_{n-1} p_{n-1}^\alpha(t) + \mu_{n+1} p_{n+1}^\alpha(t) - (\lambda_n + \mu_n) p_n^\alpha(t) \quad (A1)$$

229 for  $n \geq 0$  [39,43,53]. The rates  $\lambda_n$  and  $\mu_n$  are non-negative. The classical birth and death process  
 230 follows when  $\alpha = 1$  with state probabilities  $p_n^1(t)$ . When  $\lambda_n = \lambda$  and  $\mu_n = 0$  for all  $n$ , the  $\alpha$ -fractional  
 231 nonlinear birth and death process becomes the  $\alpha$ -fractional Poisson process [37,41,46]. There, it has  
 232 shown that  $N_\alpha(t)$  has the same probability distribution as  $N(\mathcal{T}_\alpha(t))$ , where  $N(t)$  is the classical birth  
 233 and death process which is independent of a random time process  $\mathcal{T}_\alpha(t)$ ; that is, a birth and death  
 234 process subordinated by an  $\alpha$ -stable time process.

The random time process  $\mathcal{T}_\alpha(t)$  has a distribution given by the folded solution of the fractional diffusion equation  $\partial_t^\alpha F = \partial_x^2 F$  for  $0 < \alpha \leq 2$ ,  $x \in \mathbb{R}$ ,  $t > 0$ , and subject to  $F(x, 0) = \delta(x)$  for  $0 < \alpha \leq 2$  and  $\partial_t^\alpha F(x, 0) = 0$  for  $1 < \alpha \leq 2$ , [43]. We will denote its measure by  $\nu_{\alpha,t}(ds) := P(\mathcal{T}_\alpha(t) \in ds)$ . It has a Laplace transform

$$\mathcal{L}(\nu_{\alpha,s})(r) = \int_0^\infty e^{-rt} \nu_{\alpha,t}(dt) = r^{\frac{\alpha}{2}-1} e^{-sr^{\frac{\alpha}{2}}}$$

235 and moments  $E[(\mathcal{T}_\alpha(t))^k] = \Gamma(k+1) \frac{t^{k\alpha}}{\Gamma(k\alpha+1)}$  for  $k = 1, 2, \dots$ ; [46,56].

236 Note that, the absolute values of partial derivatives of  $G$  are finite; that is,  $|\partial_{u,v,w}^{(i,j,k)} G| < \infty$  for any  
237  $i, j, k = 0, 1, 2, \dots$ . That is true since  $|u|, |v|, |w| < 1$  and the population size is finite. Thus, switching  
238 integrals with derivatives or summations below are valid.

239

## 240 Proof of the Theorem 1

We are going to show that Laplace transform of the probability generating function of the process

$$(X_1^{(1)}(\mathcal{T}_{2\alpha}(t)), X_2^{(1)}(\mathcal{T}_{2\alpha}(t)), X_3^{(1)}(\mathcal{T}_{2\alpha}(t)))$$

241 is the same as Laplace transform  $\hat{G}$  of  $G$ , that solves equation (11). From there we will conclude  
242 that the two probability distributions are the same since the probability generating function of  
243  $(X_1^{(\alpha)}(t), X_2^{(\alpha)}(t), X_3^{(\alpha)}(t))$ , by construction, is also a solution to the Cauchy problem in equation (11).

244 From equation (11), the Laplace transform  $\hat{G}$  is the solution of

$$\begin{aligned} s^\alpha \hat{G}^{(\alpha)} - s^{\alpha-1} u^{i_0} v^{j_0} w^{k_0} &= \mu N(u-1) \hat{G}^{(\alpha)} + \mu(1-u) \partial_u \hat{G}^{(\alpha)} + (\delta w + \mu - (\delta + \mu)v) \partial_v \hat{G}^{(\alpha)} \\ &\quad + (\sigma + \mu)(1-w) \partial_w \hat{G}^{(\alpha)} + \beta \frac{w}{N} (v-u) \partial_{uw} \hat{G}^{(\alpha)} \end{aligned} \quad (\text{A2})$$

Let  $H^{(\alpha)}(u, v, w, t)$  be the probability generating function of the state probabilities

$$q_{(i,j,k)}^{(\alpha)}(t) = P((X_1^{(1)}(\mathcal{T}_{2\alpha}(t)), X_2^{(1)}(\mathcal{T}_{2\alpha}(t)), X_3^{(1)}(\mathcal{T}_{2\alpha}(t))) = (i, j, k) |$$

$$(X_1^{(1)}(\mathcal{T}_{2\alpha}(0)), X_2^{(1)}(\mathcal{T}_{2\alpha}(0)), X_3^{(1)}(\mathcal{T}_{2\alpha}(0))) = (i_0, j_0, k_0)).$$

245 That means that

$$\begin{aligned} H^{(\alpha)}(u, v, w, t) &= E(u^{X_1^{(1)}(\mathcal{T}_{2\alpha}(t))} v^{X_2^{(1)}(\mathcal{T}_{2\alpha}(t))} w^{X_3^{(1)}(\mathcal{T}_{2\alpha}(t))}) \\ &= \sum_i \sum_j \sum_k u^i v^j w^k q_{(i,j,k)}^{(\alpha)}(t) \\ &= \sum_i \sum_j \sum_k u^i v^j w^k \int_0^\infty p_{(i,j,k)}^{(1)}(s) \nu_{2\alpha,t}(ds) \\ &= \int_0^\infty \left( \sum_i \sum_j \sum_k u^i v^j w^k p_{(i,j,k)}^{(1)}(s) \right) \nu_{2\alpha,t}(ds) \\ &= \int_0^\infty G^{(1)}(u, v, w, s) \nu_{2\alpha,t}(ds). \end{aligned}$$

246 Thus the Laplace transform of the probability generating function  $H^{(\alpha)}$  is given by

$$\begin{aligned} \hat{H}^{(\alpha)}(u, v, w, r) &= \int_0^\infty e^{-rt} \int_0^\infty G^{(1)}(u, v, w, s) \nu_{2\alpha,t}(ds) dt \\ &= r^{\alpha-1} \int_0^\infty G^{(1)}(u, v, w, s) e^{-sr^\alpha} ds \\ &= r^{\alpha-1} \hat{G}^{(1)}(u, v, w, r^\alpha) \end{aligned}$$

<sup>247</sup> Now, the Laplace transform of the probability generating function of the process  
<sup>248</sup>  $(X_1^{(1)}(t), X_2^{(1)}(t), X_3^{(1)}(t))$  also solves (A2) when  $\alpha = 1$  which is

$$s\hat{G}^{(1)} - u^{i_0}v^{j_0}w^{k_0} = \mu N(u-1)\hat{G}^{(1)} + \mu(1-u)\partial_u\hat{G}^{(1)} + (\delta w + \mu - (\delta + \mu)v)\partial_v\hat{G}^{(1)} + (\sigma + \mu)(1-w)\partial_w\hat{G}^{(1)} + \beta\frac{w}{N}(v-u)\partial_{uw}\hat{G}^{(1)}. \quad (\text{A3})$$

<sup>249</sup> If we substitute with  $s = r^\alpha$  in equation (A3) and multiply both sides by  $r^{\alpha-1}$  we get

$$r^\alpha\hat{H}^{(\alpha)} - r^{\alpha-1}u^{i_0}v^{j_0}w^{k_0} = \mu N(u-1)\hat{H}^{(\alpha)} + \mu(1-u)\partial_u\hat{H}^{(\alpha)} + (\delta w + \mu - (\delta + \mu)v)\partial_v\hat{H}^{(\alpha)} + (\sigma + \mu)(1-w)\partial_w\hat{H}^{(\alpha)} + \beta\frac{w}{N}(v-u)\partial_{uw}\hat{H}^{(\alpha)} \quad (\text{A4})$$

<sup>250</sup> which is the same as equation (A2). This completes the proof.

<sup>251</sup>

## <sup>252</sup> Proof of Lemma 1

Starting on the S-axis when  $E(0) = I(0) = 0$  and  $1 \geq S(0) = S_0 \geq 0$ , then

$$S(t) = t^\alpha E_{\alpha,\alpha+1}(-\mu t^\alpha)(\mu) + E_{\alpha,1}(-\mu t^\alpha)S_0 \geq 0$$

since  $\mu > 0$  and  $t \geq 0$ . Starting on the E-axis when  $S(0), I(0) = 0$  and  $E(0) = E_0 \geq 0$ , then

$$E(t) = E_{\alpha,1}(-(\mu + \delta)t^\alpha)E_0 \geq 0$$

Starting on the I-axis when  $S(0), E(0) = 0$  and  $I(0) = I_0 \geq 0$ , then

$$I(t) = E_{\alpha,1}(-(\mu + \sigma)t^\alpha)I_0 \geq 0$$

<sup>253</sup> Thus, all axes are positive invariant, for  $S(0), E(0), I(0) \geq 0$ .

If the solution of the system is leaving through the positive quadrant of the E-I plane, then  $S(t_e) = 0$ , and  $E(t_e)$  and  $I(t_e) > 0$  for some  $t_e > 0$  such that  $S(t) \leq S(t_e)$ , for all  $t > t_e$ . But,  $D_*^\alpha S|_{t=t_e} = \mu > 0$ . By the generalized mean value theorem

$$S(t) = S(t_e) + \frac{1}{\Gamma(\alpha)}D_*^\alpha S(\tau)(t - t_e)^\alpha$$

for some  $t_e \leq \tau < t$ , then  $S(t) > S(t_e)$  contradicting the original statement. The same argument could be used for the positive quadrant of the S-I plane with  $D_*^\alpha E|_{t=t_e} = \beta S(t_e)I(t_e) > 0$  and for the positive quadrant of the E-S plane with  $D_*^\alpha I|_{t=t_e} = \alpha E(t_e) > 0$ .

To show that  $S(t) + E(t) + I(t) \leq 1$  for all  $t > 0$ , if  $S(0) + E(0) + I(0) \leq 1$ ,

$$\begin{aligned} D_*^\alpha(S + E + I) &= \mu - \mu(S + E + I) - \sigma I \\ &\leq \mu - \mu(S + E + I) \end{aligned} \quad (\text{A5})$$

Thus,

$$\begin{aligned} S(t) + E(t) + I(t) &\leq t^\alpha E_{\alpha,\alpha+1}(-\mu t^\alpha)\mu + E_{\alpha,1}(-\mu t^\alpha)(S(0) + E(0) + I(0)) \\ &\leq t^\alpha E_{\alpha,\alpha+1}(-\mu t^\alpha)\mu + E_{\alpha,1}(-\mu t^\alpha) = 1 \end{aligned} \quad (\text{A6})$$

<sup>254</sup> by equation (7).

<sup>255</sup>

## <sup>256</sup> Proof of Lemma 2

For the local stability of a disease-free equilibrium, we must evaluate the Jacobian matrix at  $DFE \equiv (1, 0, 0)$

$$J(DFE) = \begin{bmatrix} -\mu & 0 & -\beta \\ 0 & -(\mu + \delta) & \beta \\ 0 & \delta & -(\mu + \sigma) \end{bmatrix}$$

The eigenvalues of the matrix  $J$  are,

$$\begin{aligned} \lambda_1 &= -\mu, \\ \lambda_2 &= \frac{-(\delta + 2\mu + \sigma) - \sqrt{\Delta}}{2}, \\ \lambda_3 &= \frac{-(\delta + 2\mu + \sigma) + \sqrt{\Delta}}{2}, \end{aligned}$$

where  $\Delta = \delta^2 + 4\delta\beta - 2\delta\sigma + \sigma^2$ . From this it is clear that  $\lambda_1$  is negative and since

$$\Delta = \delta^2 + 4\delta\beta - 2\delta\sigma + \sigma^2 = (\delta - \sigma)^2 + 4\delta\beta > 0$$

then  $\lambda_2$  and  $\lambda_3$  are real-valued numbers. Hence  $\lambda_2 < 0$ . But,  $\lambda_3 < 0$  is true when

$$\frac{-(\delta + 2\mu + \sigma) + \sqrt{\delta^2 + 4\delta\beta - 2\delta\sigma + \sigma^2}}{2} < 0$$

257 which is equivalent to  $\beta\delta < (\mu + \sigma)(\mu + \delta)$ , proving the first part.

The Jacobian matrix calculated at  $EE$  is given by

$$J(EE) = \begin{bmatrix} -\mu R_0 & 0 & -\beta \frac{1}{R_0} \\ \mu(R_0 - 1) & -(\mu + \delta) & \beta \frac{1}{R_0} \\ 0 & \delta & -(\mu + \sigma) \end{bmatrix}$$

which has a characteristic polynomial,

$$-\lambda^3 - \lambda^2[(\mu + \delta) + (\mu + \sigma) + \mu R_0] - \lambda[\mu R_0(2\mu + \delta + \sigma)] + \mu(R_0 - 1)(\mu + \sigma)(\mu + \delta).$$

Because that polynomial has a degree of 3, we choose to test the Routh-Hurwitz conditions to see if  $EE$  is stable.

$$a_1 = \mu R_0 + (2\mu + \delta + \sigma) > 0$$

$$a_3 = \mu(R_0 - 1)(\mu + \sigma)(\mu + \delta) > 0$$

With these conditions we check that the determinant,  $D_2 > 0$ .

$$\begin{aligned} D_2 &= a_1 a_2 - a_3 = (\mu R_0 + 2\mu + \delta + \sigma)(\mu R_0(2\mu + \delta + \sigma)) - (\mu(R_0 - 1)(\mu + \sigma)(\mu + \delta)) \\ &= \mu[\mu R_0^2(2\mu + \delta + \sigma) + (2\mu + \delta + \sigma)^2 R_0 - R_0(\mu + \sigma)(\mu + \delta) + (\mu + \sigma)(\mu + \delta)] \\ &= \mu[\mu R_0^2(2\mu + \delta + \sigma) + (\mu + \sigma)^2 R_0 + (\mu + \delta)^2 R_0 + (\mu + \sigma)(\mu + \delta)R_0 + (\mu + \sigma)(\mu + \delta)] > 0 \end{aligned}$$

258 From this, all Routh-Hurwitz conditions are met and all the eigenvalues of the Jacobian matrix at  
259  $EE$  are negative, meaning that  $|Re(\lambda_k)| < 0$ ,  $k = 1, 2, 3$ .

## 260 Appendix B. Data Sets and Parameter Estimation

### 261 Appendix B.1. New York

262 Monthly reported infections of measles from September 1961 to January 1963 in New York city  
 263 are given in table A1. Parameter estimation of Measles New York data from September 1961 to January  
 264 1963 using both ODE model and FDE model. The estimated parameters values for the classical ODE  
 265 model are  $(\mu, \beta, \delta, \sigma) = (0.0028, 119.22, 16.73, 10.19)$  with the sum of square error,  $SSE = 1.29 \times 10^6$   
 266 and for the FDE model are  $(\alpha, \mu, \beta, \delta, \sigma) = (0.99, 0.0029, 116.34, 19.39, 10.37)$  with the sum of square  
 267 error,  $SSE = 1.34 \times 10^6$ .

**Table A1.** Reported infections of measles from September 1961 to January 1963 in New York, US.

Year	Months	Cases	Year	Months	Cases	Year	Months	Cases
1961	September	109	1962	March	5839	1962	September	58
1961	October	123	1962	April	7875	1962	October	86
1961	November	383	1962	May	6555	1962	November	125
1961	December	1043	1962	June	2866	1962	December	145
1962	January	1725	1962	July	1075	1963	January	184
1962	February	3056	1962	August	266			

### 268 Appendix B.2. London

269 Biweekly reported infections of measles in 1961 in London, United Kingdom are given in table  
 270 A2. Parameter estimation of measles Portsmouth data in 1961 using both ODE model and FDE  
 271 model. The estimated parameters values for the classical ODE model are  $(\mu, \beta, \delta, \sigma) = (6.79 \times$   
 272  $10^{-4}, 153.44, 1.99, 4.27)$  with the sum of square error,  $SSE = 2.01 \times 10^6$  and for the FDE model are  
 273  $(\alpha, \mu, \beta, \delta, \sigma) = (0.99, 8.53 \times 10^{-4}, 62.89, 5.37, 4.95)$  with the sum of square error,  $SSE = 4.37 \times 10^6$ .

**Table A2.** Biweekly reported measles infections in 1961 in London, UK.

Year	Weeks	Cases									
1961	0	1636	1961	14	5374	1961	28	514	1961	42	89
1961	2	2700	1961	16	4272	1961	30	375	1961	44	87
1961	4	2639	1961	18	2322	1961	32	265	1961	46	73
1961	6	4805	1961	20	1810	1961	34	199	1961	48	70
1961	8	6543	1961	22	1409	1961	36	121	1961	50	59
1961	10	6389	1961	24	1037	1961	38	86	1961	52	45
1961	12	5545	1961	26	767	1961	40	76			

### 274 Appendix B.3. Portsmouth

275 Biweekly reported infections of measles in 1961 in Portsmouth, United Kingdom are given in table  
 276 A3. Parameter estimation of measles Portsmouth data in 1961 using both ODE model and FDE model.  
 277 The estimated parameters values for the classical ODE model are  $(\mu, \beta, \delta, \sigma) = (10^{-6}, 228.61, 0.46, 3.33)$   
 278 with the sum of square error,  $SSE = 4.57 \times 10^4$  and for the FDE model are  $(\alpha, \mu, \beta, \delta, \sigma) = (0.88, 2.56 \times$   
 279  $10^{-4}, 278.72, 1.52, 5.24)$  with the sum of square error,  $SSE = 3.22 \times 10^4$ .

**Table A3.** Biweekly reported infections of measles in 1961 in Portsmouth, UK.

weeks	2	4	6	8	10	12	14	16	18	20	22	24	26	28	30	32
cases	4	30	58	174	310	407	640	847	555	523	337	242	144	91	29	21
weeks	34	36	38	40	42	44	46	48	50	52						
cases	25	28	13	5	2	1	2	0	2	0						

280 *Appendix B.4. Parameter Estimations***Table A4.** Comparison between the classical ODE model and FDE model using different data sets

Data	Model	Estimated Parameters, $(\alpha, \mu, \beta, \delta, \sigma)$	SSE
New York	ODE	$(Na, 0.0028, 119.22, 16.73, 10.19)$	$1.29 \times 10^6$
	FDE	$(0.99, 0.0029, 116.34, 19.39, 10.37)$	$1.34 \times 10^6$
Portsmouth	ODE	$(Na, 10^{-6}, 228.61, 0.46, 3.33)$	$4.57 \times 10^4$
	FDE	$(0.88, 2.52 \times 10^{-4}, 278.72, 1.52, 5.24)$	$3.22 \times 10^4$
London	ODE	$(Na, 6.79 \times 10^{-4}, 153.44, 1.99, 4.27)$	$2.01 \times 10^6$
	FDE	$(0.99, 8.52 \times 10^{-4}, 62.89, 5.37, 4.95)$	$4.36 \times 10^6$

281

282 **References**

1. Bernoulli, D. Essai d'une nouvelle analyse de la mortalité causée par la petite vérole. In *Mém Math Phys Acad Roy Sci Paris*; 1766; Vol. 1, pp. 1–45.
2. Ross, R. An Application of the Theory of Probabilities to the Study of a priori Pathometry. Part I. *Proceedings of the Royal Society A: Mathematical, Physical and Engineering Sciences* **1916**, *92*, 204–230. doi:10.1098/rspa.1916.0007.
3. Brownlee, J. Certain Aspects of the Theory of Epidemiology in Special Relation to Plague. *Proceedings of the Royal Society of Medicine* **1918**, *11*, 85–132.
4. Greenwood, M.; Yule, G.U. An Inquiry into the Nature of Frequency Distributions Representative of Multiple Happenings with Particular Reference to the Occurrence of Multiple Attacks of Disease or of Repeated Accidents. *Journal of the Royal Statistical Society* **1920**, *83*, 255. doi:10.2307/2341080.
5. Kermack, W.O.; McKendrick, A.G. A Contribution to the Mathematical Theory of Epidemics. *Proceedings of the Royal Society A: Mathematical, Physical and Engineering Sciences* **1927**. doi:10.1098/rspa.1927.0118.
6. Soper, H.E. The Interpretation of Periodicity in Disease Prevalence. *Journal of the Royal Statistical Society* **1929**, *92*, 34. doi:10.2307/2341437.
7. Greenwood, M. On the Statistical Measure of Infectiousness. *The Journal of hygiene* **1931**, *31*, 336–51.
8. Greenwood, M. The statistical study of infectious diseases. *Journal of the Royal Statistical Society. Series A (General)* **1946**, *109*, 85–110.
9. M. S. Bartlett. Some Evolutionary Stochastic Processes. *Journal of the Royal Statistical Society. Series B (Methodological)* **1949**, *11*, 211–229.
10. Bailey, N.T.J. The Total Size of a General Stochastic Epidemic. *Biometrika* **1953**, *40*, 177. doi:10.2307/2333107.
11. Bailey, N.T.J. *The mathematical theory of infectious diseases and its applications*; Griffin, 1975; p. 413.
12. Anderson, R.M. *The Population dynamics of infectious diseases : theory and applications*; 1982.
13. Hethcote, H.W. The Mathematics of Infectious Diseases. *SIAM Review* **2005**. doi:10.1137/s0036144500371907.
14. Keeling, M.J.; Danon, L. Mathematical modelling of infectious diseases, 2009. doi:10.1093/bmb/ldp038.
15. Anderson, R.M.; May, R.M. *Infectious Diseases of Humans: Dynamics and Control* (Oxford Univ. Press, Oxford) **1991**.
16. Castillo-Chavez, C.; Blower, S.; van den Driessche, P.; Kirschner, D.; Abdul-Aziz, Y. *Mathematical Approaches for Emerging and Reemerging Infectious Diseases*; 2002. doi:10.1007/978-1-4613-0065-6.
17. Temime, L.; Hejblum, G.; Setbon, M.; Valleron, A. The rising impact of mathematical modelling in epidemiology: antibiotic resistance research as a case study. *Epidemiology and Infection* **2008**, *136*, 289. doi:10.1017/S0950268807009442.
18. Fisman, D.N.; Hauck, T.S.; Tuite, A.R.; Greer, A.L. An IDEA for Short Term Outbreak Projection: Nearcasting Using the Basic Reproduction Number. *PLoS ONE* **2013**, *8*, e83622. doi:10.1371/journal.pone.0083622.
19. Ahmed, E.; Elgazzar, A.S. On fractional order differential equations model for nonlocal epidemics. *Physica A: Statistical Mechanics and its Applications* **2007**. doi:10.1016/j.physa.2007.01.010.

320 20. Demirci, E.; Unal, A.; Özalp, N. A fractional order SEIR model with density dependent death rate. *Hacettepe*  
321 *Journal of Mathematics and Statistics* **2011**.

322 21. Al-Sheikh, S.A. Modeling and Analysis of an SEIR Epidemic Model with a Limited Resource for Treatment  
323 Modeling and Analysis of an SEIR Epidemic Model with a Limited Resource for Treatment Modeling  
324 and Analysis of an SEIR Epidemic Model with a Limited Resource for Treatment. *Type : Double Blind Peer*  
325 *Reviewed International Research Journal Publisher: Global Journals Inc* **2012**, 12.

326 22. Diethelm, K. A fractional calculus based model for the simulation of an outbreak of dengue fever. *Nonlinear*  
327 *Dynamics* **2013**. doi:10.1007/s11071-012-0475-2.

328 23. Li, J.; Cui, N. Dynamic analysis of an SEIR model with distinct incidence for exposed and infectives. *The*  
329 *Scientific World Journal* **2013**, 2013, 1–5. doi:10.1155/2013/871393.

330 24. El-Shahed, M.; El-Naby, F.A. Fractional calculus model for childhood diseases and vaccines. *Applied*  
331 *Mathematical Sciences* **2014**, 8, 4859–4866. doi:10.12988/ams.2014.4294.

332 25. Dold, E.A.; Eckmann, B.; Accola, R.D.M. *Lecture Notes in Mathematics Springer-Verlag*; 1975.

333 26. Almeida, R.; Brito da Cruz, A.M.; Martins, N.; Monteiro, M.T.T. An epidemiological MSEIR model  
334 described by the Caputo fractional derivative. *International Journal of Dynamics and Control* **2018**, pp. 1–14.  
335 doi:10.1007/s40435-018-0492-1.

336 27. Area, I.; Batarfi, H.; Losada, J.; Nieto, J.J.; Shammakh, W.; Torres, Á. On a fractional order Ebola epidemic  
337 model. *Advances in Difference Equations* **2015**. doi:10.1186/s13662-015-0613-5.

338 28. Haggett, P. *The geographical structure of epidemics*; Clarendon Press, 2000; p. 149.

339 29. Bjørnstad, O.N.; Finkenstädt, B.F.; Grenfell, B.T. Dynamics of Measles Epidemics : Estimating Scaling of.  
340 *Ecological Monographs* **2002**, 72, 169–184.

341 30. Yingcun Xia.; Ottar N. Bjørnstad.; Bryan T. Grenfell. Measles Metapopulation Dynamics: A Gravity Model  
342 for Epidemiological Coupling and Dynamics. *The American Naturalist* **2004**. doi:10.1086/422341.

343 31. Greenwood, P.E.; Gordillo, L.F. Stochastic epidemic modeling. In *Mathematical and Statistical Estimation*  
344 *Approaches in Epidemiology*; 2009; pp. 31–52. doi:10.1007/978-90-481-2313-1\_2.

345 32. Vasilyeva, O.; Oraby, T.; Lutscher, F. Aggregation and environmental transmission in Chronic Wasting  
346 Disease. *Mathematical Biosciences and Engineering* **2015**, 12. doi:10.3934/mbe.2015.12.209.

347 33. Aranda, D.F.; Trejos, D.Y.; Valverde, J.C. A fractional-order epidemic model for bovine Babesiosis disease  
348 and tick populations. *Open Physics* **2017**, 15, 360–369. doi:10.1515/phys-2017-0040.

349 34. Angstmann, C.; Henry, B.; McGann, A. A Fractional-Order Infectivity and Recovery SIR Model. *Fractal and*  
350 *Fractional* **2017**, 1, 11. doi:10.3390/fractfrac1010011.

351 35. Sardar, T.; Rana, S.; Chattopadhyay, J. A mathematical model of dengue transmission with  
352 memory. *Communications in Nonlinear Science and Numerical Simulation* **2015**, 22, 511–525.  
353 doi:10.1016/j.cnsns.2014.08.009.

354 36. Saeedian, M.; Khalighi, M.; Azimi-Tafreshi, N.; Jafari, G.R.; Ausloos, M. Memory effects on epidemic  
355 evolution: The susceptible-infected-recovered epidemic model. *Physical Review E* **2017**, [1703.03191].  
356 doi:10.1103/PhysRevE.95.022409.

357 37. Laskin, N. Fractional Poisson process **2003**, 8, 201–213. doi:10.1016/S1007-5704(03)00037-6.

358 38. UCHAIKIN, V.V.; CAHOY, D.O.; SIBATOV, R.T. FRACTIONAL PROCESSES: FROM POISSON  
359 TO BRANCHING ONE. *International Journal of Bifurcation and Chaos* **2008**, 18, 2717–2725.  
360 doi:10.1142/s0218127408021932.

361 39. Orsingher, E.; Polito, F.; Sakhno, L. Fractional Non-Linear, Linear and Sublinear Death Processes. *Journal of*  
362 *Statistical Physics* **2010**, 141, 68–93. doi:10.1007/s10955-010-0045-2.

363 40. Orsingher, E.; Polito, F. Fractional pure birth processes. *Bernoulli* **2010**, 16, 858–881. doi:10.3150/09-bej235.

364 41. Meerschaert, M.M.; Nane, E.; Vellaisamy, P. The fractional poisson process and the inverse stable  
365 subordinator. *Electronic Journal of Probability* **2011**, 16, 1600–1620. doi:10.1214/EJP.v16-920.

366 42. Garra, R.; Polito, F. A note on fractional linear pure birth and pure death processes in epidemic models.  
367 *Physica A: Statistical Mechanics and its Applications* **2011**, 390, 3704–3709. doi:10.1016/j.physa.2011.06.005.

368 43. Orsingher, E.; Polito, F. On a fractional linear birth-death process. *Bernoulli* **2011**, 17, 114–137.  
369 doi:10.3150/10-bej263.

370 44. Orsingher, E.; Ricciuti, C.; Toaldo, B. Population models at stochastic times. *Advances in Applied Probability*  
371 **2016**, 48, 481–498. doi:10.1017/apr.2016.11.

372 45. Di Crescenzo, A.; Martinucci, B.; Meoli, A. A fractional counting process and its connection with the  
373 poisson process. *Alea* **2016**, *13*, 291–307.

374 46. Kumar, A.; Leonenko, N.; Pichler, A. Fractional Risk Process in Insurance **2018**. pp. 1–25, [1808.07950].

375 47. Podlubny, I. Geometric and Physical Interpretation of Fractional Integration and Fractional Differentiation  
376 **2008**. pp. 1–18, [arXiv:arXiv:math/0110241v1].

377 48. Özalp, N.; Demirci, E. A fractional order SEIR model with vertical transmission **2011**. *54*, 1–6.  
378 doi:10.1016/j.mcm.2010.12.051.

379 49. Earn, D.J.; Rohani, P.; Bolker, B.M.; Grenfell, B.T. A simple model for complex dynamical transitions in  
380 epidemics. *Science* **2000**. doi:10.1126/science.287.5453.667.

381 50. Allen, L.J.S. *Stochastic Population and Epidemic Models*; 2015. doi:10.1007/978-3-319-21554-9.

382 51. Allen, L. *An Introduction to Stochastic Processes with Applications to Biology, Second Edition*; 2018.  
383 doi:10.1201/b12537.

384 52. Di Crescenzo, A.; Meoli, A. On a fractional alternating Poisson process. *AIMS Mathematics*, pp. 212–224.  
385 doi:10.3934/math.2016.3.212.

386 53. Konno, H.; Pázsit, I. Fractional Linear Birth-Death Stochastic Process—An Application of Heun’s  
387 Differential Equation. *Reports on Mathematical Physics* **2018**, *82*, 1–20. doi:10.1016/S0034-4877(18)30062-4.

388 54. Demirci, E.; Özalp, N. A method for solving differential equations of fractional order. *Journal of  
389 Computational and Applied Mathematics* **2012**, *236*, 2754–2762. doi:10.1016/j.amc.2015.05.049.

390 55. Mandelbrot, B.; Taylor, H.M. On the Distribution of Stock Price Differences. *Operations Research* **1967**,  
391 *15*, 1057–1062. doi:10.1287/opre.15.6.1057.

392 56. Piryatinska, A.; Saichev, A.; Woyczynski, W. Models of anomalous diffusion: the subdiffusive case. *Physica  
393 A: Statistical Mechanics and its Applications* **2005**, *349*, 375–420. doi:10.1016/j.physa.2004.11.003.